Desalination and Water Treatment
www.deswater.com

doi: 10.5004/dwt.2021.27447

234 (2021) 58–67
September

UV-L/sulfite advanced reduction process as an efficient method for chlorate reduction in water

Nasr Bensalah[a,*], Ahmed Abdel-Wahab[b]

[a]*Department of Chemistry and Earth Sciences, College of Arts and Sciences, Qatar University, P.O. Box: 2713, Doha, Qatar, Tel. +974-4403-6540; email: nasr.bensalah@qu.edu.qa*
[b]*Chemical Engineering Program, Texas A&M University at Qatar, P.O. Box: 23874, Doha, Qatar, email: ahmed.abdel-wahab@qatar.tamu.edu*

Received 11 December 2020; Accepted 21 May 2021

ABSTRACT

The efficient reduction of disinfection by-products (DBPs) is currently a major challenge in water treatment facilities due to their high toxicity to human health and long-time residence in the environment. In this work, an advanced reduction process (ARP) that combines ultraviolet light irradiation using a low-pressure mercury lamp and sulfite reducing agent (UV-L/sulfite) was investigated for the reduction of chlorate, as a model of inorganic chlorination DBPs. The UV-L/sulfite ARP was much more effective than single processes such as sulfite alone or UV irradiation alone. The higher efficiency of UV-L/sulfite is due to the formation of free reducing radical species (sulfite anion radical ($SO_3^{\bullet -}$), hydrated electron (e^-_{aq}), and hydrogen atom ($H^\bullet$)). Effects of sulfite dose, initial pH, initial chlorate concentration, and UV-L light dose on the rate and extent of chlorate reduction were evaluated. Chlorate reduction was notable only in an acidic pH environment and its reduction rate was very slow at neutral and basic pH values. Increasing sulfite dose up to 180 mg/L led to increasing the efficiency and accelerated the rate of chlorate reduction. Increasing UV-light intensity up to 670 µW/cm^2 (10 mg/L chlorate and 180 mg/L sulfite) improved the efficiency and accelerated the chlorate reduction rate by producing large amounts of free-reducing radicals. The major reaction product from chlorate reduction by UV-L/sulfite ARP was chloride with the formation of free chlorine as an intermediate and no chlorite was detected. The presence of $SO_3^{\bullet -}$, e^-_{aq}, and $H^\bullet$ scavengers affected the efficiency of UV-L/sulfite ARP. A decrease of chlorate reduction yield was observed in presence of dissolved oxygen, nitrite, or nitrate confirming the contribution of $SO_3^{\bullet -}$, e^-_{aq}, and $H^\bullet$ in the mechanism of chlorate reduction. However, the presence of Fe^{3+} enhanced chlorate reduction yield due to the formation of additional $SO_3^{\bullet -}$ radicals from the photodecomposition of Fe(III)-HSO_3^- complexes. The mechanism of chlorate reduction into chloride involves oxygen atom-abstraction and consecutive reactions with the formation of chlorite, hypochlorite as intermediates. These results point to conclude that UV-L/sulfite ARP has a great potential to be applied in water treatment to control the formation of undesirable DBPs.

Keywords: Disinfection by-products; Chlorate; Advanced reduction processes; UV-L/sulfite process; sulfite anion radicals

1. Introduction

Oxidation–reduction reactions are the primary way in which water treatment processes destroy environmental contaminants. Although many oxidation–reduction reactions are thermodynamically feasible, most do not occur at reasonable rates under normal conditions of temperature and pressure. A group of treatment processes called

---

[*] Corresponding author.

advanced oxidation processes (AOPs) overcome this problem by producing highly reactive hydroxyl radicals ($HO^\bullet$) that are responsible for oxidizing contaminants to environmentally benign products [1–3]. Hydroxyl radicals are often produced in AOPs by combining a reagent (e.g., hydrogen peroxide, ozone) with a physical activation method (e.g., ultraviolet light, ultrasound) [4,5]. The reactivity of the $HO^\bullet$ radical is due to short life-time and chemical instability by the presence of unpaired electrons [6–8]. Oxidizing free radicals remove an electron from the contaminant being oxidized in order to form a paired set of electrons. Applications of free radical chemistry for treating water, wastewater and hazardous wastes have been limited almost entirely to applying oxidizing free radicals such as $HO^\bullet$ radical in AOPs. However, there are also reductive free radicals that react with contaminants by donating an unpaired electron to them. The hydrogen radical ($H^\bullet$) and hydrated electron (e^-_{aq}) is an example of a reducing free radical [8,9]. Reductive free radicals can also be formed and applied to water treatment applications that require reduction. Examples of oxidized contaminants that are destroyed by reductive treatment include perchlorate, chlorate, chlorite, free chlorine, chromate, chlorinated organics, nitrate, nitrite, arsenate, selenate, bromate, and a number of radionuclides. Advanced reduction processes (ARPs) take the approach of many AOPs of combining reagents and activating methods to produce reducing free radicals, rather than an oxidizing free radical. ARPs have been proposed for destroying oxidized contaminants by producing reductive free radicals [10–19].

The most promising ARP identified so far is the combination of sulfite with low-pressure ultraviolet light (UV-L) [20–23]. This ARP is the most promising primarily because it appears to have the greatest ability to effectively destroy contaminants. It is also attractive since it could be developed more rapidly, and it could use available UV-L dosing systems that are currently being used to disinfect water and wastewater. Nearly complete removal of nitrate at the earliest sampling time was observed at moderate to high pH with the sulfite/UV-L ARP. The sulfite/UV-L ARP was also able to destroy perchlorate to a 17% extent [12]. Although this extent of removal is small in itself, it is much higher than the perchlorate destruction achieved by other chemical reductants [24]. A mechanism for the ability of the sulfite/UV-L ARP to successfully degrade oxidized compounds is that UV light converts the sulfite into highly reactive free radicals [11,21,25]. Sulfite solutions absorb UV light with a maximum near 276 nm [26,27], so there is a source of energy imparted to the sulfite ions that could be used to produce reactive free radicals. Further evidence for the production of highly reactive reductants in irradiated sulfite solutions is that they produce hydrogen [28] and react with oxygen more rapidly than non-irradiated solutions. The increased ability of irradiated sulfite solutions to reduce chemicals is generally explained by the production of the aqueous electron (e^-_{aq}) [8,29,30], which is a highly reactive reductant. An alternative mechanism is that irradiation of sulfite solutions results in the formation of the sulfur dioxide radical anion ($SO_2^{\bullet-}$), which is another highly reactive reductant [31]. Regardless of the species being formed, irradiation of sulfite solutions produces free radicals that promote redox reactions that can be used to destroy oxidized contaminants.

Chlorate (ClO_3^-) is one of the oxidized contaminants detected as disinfection by-products (DBPs) in water disinfection by chlorine and its derivatives [32,33]. Chlorate was formed during water disinfection by chlorine [34–36], hypochlorites [37–39], chlorine dioxide [40,41], and electro-chlorination [42,43]. The chlorates and other DBPs were detected in swimming pools, bathing water, drinking water, and groundwater [44–47]. Also, wastewater discharges from Chlor-alkali plants and the sodium chlorate manufacturing industry are usually contaminated with chlorate [48,49]. Recent studies showed that chlorates cause deleterious human health concerns [32,50–55]. The regulation of chlorate level to a maximum contaminant level (MCL) of 1 mg/L in drinking water is under progress in many countries over the world including Europe, USA, and Canada [54,56–59].

Several treatment methods have been applied to remove chlorate from water, these include biological, physical, chemical, and combined methods [60–64]. Although several biological methods were successful to reduce chlorate into chloride, they took a very long time to reach the desired reduction of chlorate [65,66]. In addition, only partial reduction of chlorate was achieved by chemical reduction using zero-valent iron, carbon-supported iridium catalyst, nickel catalysts, and ferrous iron, Fe^{2+} [60,62,67–69]. Recently, Jung et al. [70] investigated the reduction of chlorate using dithionite ($S_2O_4^{2-}$)/UV ARP. Very promising results were obtained and $S_2O_4^{2-}$/UV system was able to reduce chlorate into chloride. However, the complete reduction of chlorate was achieved at pH in the range of 3–4 and a high dose of dithionite was required to achieve high efficiency of chlorate reduction. The authors claimed that the mechanism of degradation involved sulfite ions, among others, which are formed by the decomposition of dithionite in an acid medium.

This work aims to investigate chlorate reduction in water by UV-L/sulfite ARP and elucidate the mechanisms involved under different operating conditions and determine the conditions under which the sulfite/UV-L ARP can rapidly degrade chlorate. Although sulfite (SO_3^{2-}) is a particular anion, it will be used thereafter in this article as a general term to describe the group of sulfurous acid (H_2SO_3), bisulfite (HSO_3^-) and sulfite (SO_3^{2-}) ions. The extent of reduction was measured by the decrease of chlorate concentration and the increase of chloride concentration. Additional experiments were conducted to evaluate the effects of pH, sulfite dose, chlorate concentration, UV-L intensity, and the presence of hydrated electron (e^-_{aq}) and free radicals scavengers (dissolved oxygen (DO), nitrate, and carbonate).

2. Experimental

2.1. Chemicals

Sodium chlorate ($NaClO_3$), sodium chlorite ($NaClO_2$), sodium chloride (NaCl) were of analytical grade from Sigma-Aldrich Pty. Ltd., (Germany). Sodium sulfite (anhydrous ≥ 98.0% ACS) was received from VWR and used without any further purification. Sodium hydroxide (NaOH), sodium carbonate (Na_2CO_3), sodium nitrate ($NaNO_3$), phosphoric acid (H_3PO_4) were bought from Fisher Scientific UK Ltd., (UK).

All the aqueous solutions were prepared using deoxygenated and deionized water. Deionized water was obtained from the Millipore Milli-Q purification system (resistivity 18.2 MΩ cm, TOC ≤ 5 ppb). Deoxygenation of the solutions was carried out by purging pure nitrogen gas in the solutions for 2 h, and then keep them inside an anaerobic chamber where the photochemical experiments for chlorate reduction were conducted.

2.2. Analytical methods

Chlorates, chlorites, chlorides, and sulfates were monitored using Dionex ICS-2000 ion chromatograph equipped with EGC Eluent Generator, IonPac AS19 (4 mm × 250 mm) analytical separation column, ASRS 300–4 mm suppressor, and DS6 conductometric cell. The standard solutions were prepared by successive dilution of 50 mg/L stock solutions. The method detection limit by IC method was found to be 5, 6, 1, and 160 µg/L for chlorates, chlorites, chlorides, and sulfates, respectively. Free chlorine was analyzed using DPD colorimetric method [71]. Linear calibration curves were obtained for all the analytes with a regression factor $R^2 > 0.99$. pH was monitored using a pH-meter (SevenCompact S210, METTLER TOLEDO®). DO was measured using an oxygen probe (Extech Heavy Duty Dissolved Oxygen Meter) with automatic temperature compensation.

2.3. Photochemical experiments

Chlorate reduction experiments were performed in batch mode in a photochemical box chamber. The photochemical box chamber was accommodated inside a flexible anaerobic chamber (Coy Laboratory Products Inc., USA) under a nitrogen gas (99.99%) atmosphere equipped with an oxygen detector and a palladium catalyst STAK-PAK to ensure an oxygen-free environment. Batch kinetic experiments were performed in quartz cells (Starna 32/Q/10, Spectrosil® Quartz) fitted with a PTFE stopper with a total volume of 17 mL and 10 cm optical path length. UV irradiation of the solutions was conducted using a low-pressure mercury lamp (G64T5L/4, UV-Consulting Peschl, Germany) emitting polychromatic UV-C light with a power input of 75 W (30 W at 254 nm). The UV radiation power was monitored using a UVM-CP digital UV meter positioned in a UV-C sensor. During UV irradiation experiments, the photochemical chamber was closed to ensure safe operation and to prevent the entrance of external light. The control of the UV light intensity was possible by adjusting the distance between the lamp and the quartz cells. Chlorate reduction experiments started when the lamp was switched on. Samples were withdrawn at the desired times and directly sent to analysis. No quenching of the samples was required based on preliminary experiments confirming no reaction between sulfite and chlorate is possible.

3. Results and discussion

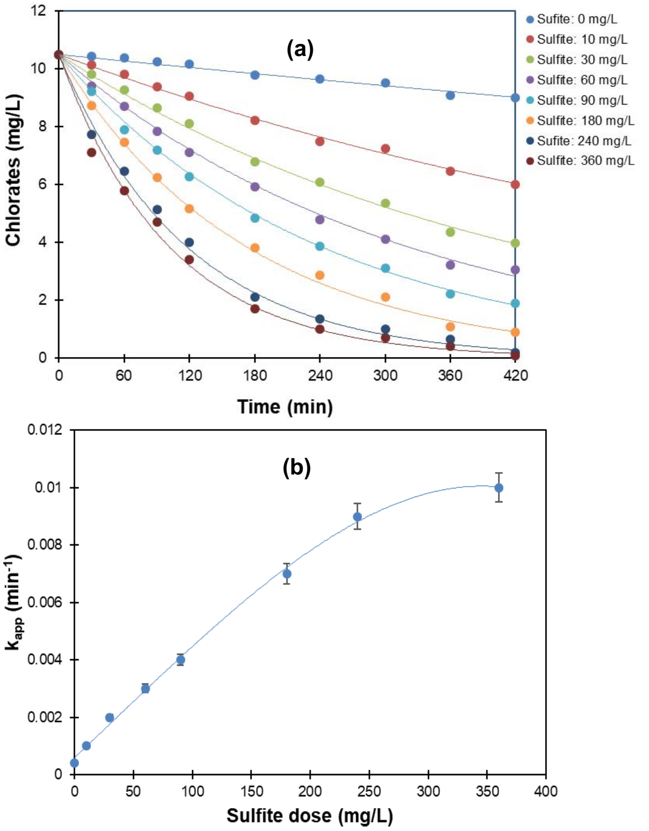

Fig. 1. Changes of (a) chlorate concentration with time at different sulfite doses, (b) changes of pseudo-first-order rate constant (k_{app}) with sulfite dose during photochemical chlorate reduction using UV-L/sulfite ARP. Experimental conditions: sulfite dose: 0–360 mg/L; initial chlorate concentration: 10.5 mg/L; initial pH = 5.4; T = 25°C; DO = 0.21 mg O_2/L; UV-L power output: 75 W; UV light intensity: 670 µW/cm^2.

Fig. 1a displays the effect of sulfite dose on the changes of chlorate concentration with time during photochemical chlorate reduction using UV-L/sulfite ARP (initial chlorate concentration: 10.5 mg/L, initial pH = 5.4, DO = 0.21 mg O_2/L). The results showed that chlorate concentration decreased with time for all the sulfite doses in the range of 0–360 mg/L. UV-L alone reduced 14.2% of initial chlorate concentration, while sulfite (360 mg/L) alone did not result in a detectable change in chlorate concentration. The increase of sulfite dose from 0 to 360 mg/L enhanced the kinetics and the yield of chlorate reduction. These results confirmed that the combined ARP system of UV-L/sulfite is very effective in chlorate reduction. It is presumed that activation of sulfite solutions with UV-L results in the formation of reductive species that are capable of destroying chlorate in water. Further discussions about the formation of radical species will be given in the subsequent sections.

All the kinetic results shown in Fig. 2a can be modeled using a pseudo-first-order kinetics model. The pseudo-first-order rate constant, k_{app}, increased linearly with the increase of sulfite dose from 0 up to 180 mg/L, with decreasing slope for sulfite doses higher than 180 mg/L (Fig. 1b). Chlorate decay yields at the end of the experiments (after 420 min) were 42.6%, 62.0%, 70.9%, 81.8%, 91.6%, 98.2%, and 99.0% for sulfite doses of 10, 30, 60, 90, 180, 240, and 360 mg/L, respectively. In addition, the times required to reach ≤1 mg/L chlorate concentration were 360, 300, and 240 min for sulfite doses 180, 240, and 360 mg/L,

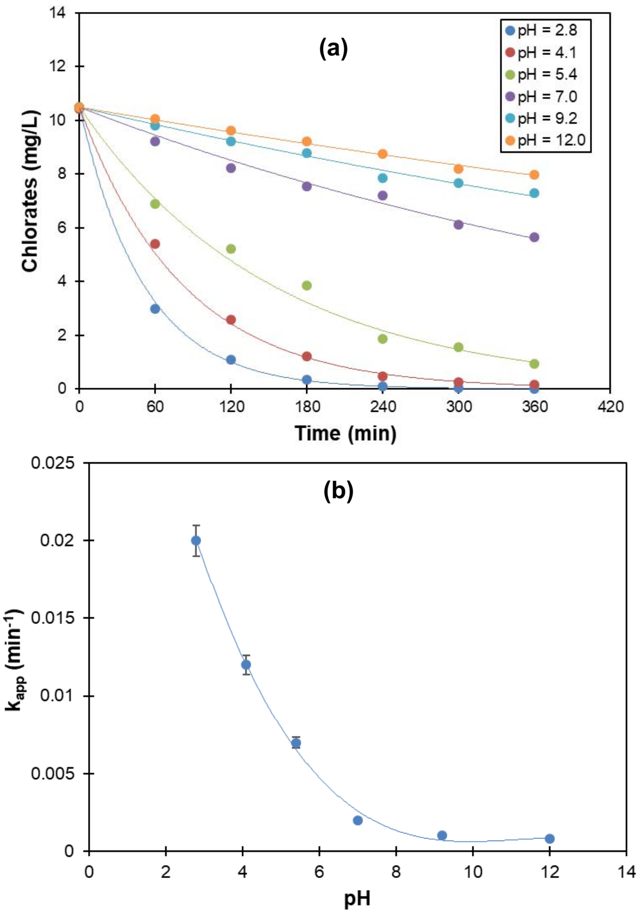

Fig. 2. Changes of (a) chlorate concentration with time at different initial pH values, (b) changes of pseudo-first-order rate constant (k_{app}) with initial pH during photochemical chlorate reduction using UV-L/sulfite ARP. Experimental conditions: sulfite dose: 180 mg/L; initial chlorate concentration: 10.5 mg/L; initial pH = 2.8–12.0; $T = 25°C$; DO = 0.21 mg O_2/L; UV-L power output: 75 W; UV light intensity: 670 µW/cm^2.

respectively. Lower sulfite doses than 180 mg/L did not achieve chlorate concentrations ≤1 mg/L. These results demonstrate that sulfite doses ≥180 are sufficient to reduce chlorate concentration to less than the proposed MCL of 1 mg/L. Higher doses than 180 mg/L are not cost-effective since they did not significantly enhance the kinetics of the reaction. This indicates that a molar ratio (sulfite/chlorate) of 18 is required to keep the chlorate concentration less than MCL within a reasonable period of time.

The oxidation–reduction photochemistry of sulfite solutions has been widely studied in atmospheric sciences, because of the importance in atmospheric chemistry of the oxidation of sulfurous acid to form sulfuric acid [72,73]. Sulfite solutions absorb UV light with a maximum in the range of 240–280 nm [74–76]. UV irradiation of sulfite solutions has been generally reported to produce three reducing radicals [Eqs. (1)–(3)]: sulfite radical anion ($SO_3^{\bullet-}$), hydrated electron (e^-_{aq}) and hydrogen atom ($H^{\bullet}$) [27,74,75,77]. The sulfite radical anion ($SO_3^{\bullet-}$) has been identified [29] and it can act as both oxidizing and reducing radically. The aqueous electron has been identified in irradiated sulfite solutions [27,30] and it is known to be a strong reductant.

$$SO_3^{2-} + h\nu \rightarrow SO_3^{\bullet-} + e^-_{aq} \tag{1}$$

$$e^-_{aq} + H^+ \rightarrow H^{\bullet} \tag{2}$$

$$SO_3^{\bullet-} + e^-_{aq} \rightarrow SO_3^{2-} \tag{3}$$

Evidence for the formation of active reductants in irradiated sulfite solutions can also be found in the production of reduced species of the target contaminant. Although the mechanisms have not been reported, irradiation of sulfite solutions by UV light has promoted their ability to form hydrogen [28], their ability to react with oxygen [78] and their ability to dehalogenation compounds [74,75].

The observed ability of the UV-L/sulfite ARP to reduce chlorate is due to the effectiveness of sulfite radical anion ($SO_3^{\bullet-}$) in reducing chlorate through an oxygen abstraction mechanism (Taube, 1982). This would produce chlorite (ClO_2^-), which in turn is reduced to chloride. The sulfate radical anion that is produced would be reduced by the aqueous electron. The following equations can explain how the oxygen abstraction mechanism would work.

$$SO_3^{2-} + h\nu \rightarrow SO_3^{\bullet-} + e^-_{aq} \tag{4}$$

$$SO_3^{\bullet-} + ClO_3^- \rightarrow SO_4^{\bullet-} + ClO_2^- \tag{5}$$

$$SO_4^{\bullet-} + e^-_{aq} \rightarrow SO_4^{2-} \tag{6}$$

Fig. 2a presents the effect of initial pH on the rate and extent of chlorate reduction using UV-L/sulfite ARP (initial chlorate concentration: 10.5 mg/L, sulfite dose: 180 mg/L, DO = 0.21 mg O_2/L). Although chlorate concentration decreased with time for all the initial pH values in the range 2.8–12.0, the kinetics were much higher in acidic conditions than that for the neutral and basic environments. The curves at low pH values followed an exponential trend confirming pseudo-first-order kinetics for the chlorate decay using UV-L/sulfite ARP. The pseudo-first-order rate constant, k_{app}, dropped rapidly with the increase of initial pH up to 7.0, then it remains invariant for pH > 7.0 as shown in Fig. 2b. Furthermore, chlorate decay is more important at pH ≤ 5.4 where chlorate concentration reached values ≤1 mg/L after 360 min. Almost complete chlorate decay was achieved under the lowest initial pH value of 2.8 after 240 min. Since the initial pH value of 5.4 is the closest to neutral conditions that enabled chlorate decay to levels less than 1 mg/L, it was selected to be used for the rest of chlorate destruction experiments to avoid any further step of pH acidification or neutralization before and after the treatment. This is might be in connection with the nature of reductive species involved in the mechanisms of chlorate decay. It was reported [74,75] that the UV photolytic decomposition of bisulfite (HSO_3^-), which is the sulfite species present in acidic pH values, forms both sulfite anion radical and a hydrogen atom ($H^•$).

$$HSO_3^- + h\nu \rightarrow SO_3^{•-} + H^• \quad (7)$$

$$SO_4^{•-} + H^• \rightarrow HSO_4^- \quad (8)$$

In contrast to reports of production of the sulfite radical anion and the aqueous electron when sulfite solutions are irradiated. Pemberton et al. [31] reported that irradiation of sulfite solutions produced the sulfur dioxide radical anion ($SO_2^{•-}$) and the hydroxyl radical ($HO^•$). Since the sulfur dioxide radical is reported to be formed by the photolytic decomposition of HSO_3^- [31], the difference in the radicals formed ($SO_3^{•-}$ or $SO_2^•$) may depend on pH, because sulfite dominates at high pH and sulfurous acid/sulfur dioxide dominates at low pH. Being stronger reducing reagent than $SO_3^{•-}$, $SO_2^•$ is more effective in reducing chlorate and higher efficiency is observed at acidic pH values [Eqs. (9)–(11)].

$$HSO_3^- + h\nu \rightarrow SO_2^• + HO^• \quad (9)$$

$$SO_2^• + ClO_3^- \rightarrow SO_3^• + ClO_2^- \quad (10)$$

$$SO_3^• + HO^• \rightarrow HSO_3^- \quad (11)$$

Fig. 3 presents the effect of the initial chlorate concentration on the changes of normalized chlorate concentration (C/C_0) with time, where C and C_0 are the chlorate concentration at an instant time t and at $t = 0$ min, respectively. Initial chlorate concentrations in the range of 3.5–21.2 mg/L were investigated while maintaining an initial sulfite/chlorate molar ratio at 18.0, DO of 0.21 mg O_2/L, and an initial pH value of 5.4. The higher is the initial chlorate concentration the slower is chlorate decay at a constant sulfite/chlorate molar ratio. The pseudo-first-order rate constant, k_{app}, decreased from 0.02 min^{-1} for the lowest initial chlorate concentration of 3.5 mg/L to 0.01, 0.006 and 0.005 min^{-1} for initial chlorate concentrations of 6.25, 10.5, and 21.2 mg/L, respectively. Complete chlorate decay was achieved for the lowest initial concentration of 3.5 mg/L, while 98.5%, 91.5%, and 86.7% of chlorate decay yields were accomplished for initial chlorate concentration of 6.25, 10.5, and 21.2 mg/L, respectively. Although (sulfite/chlorate) molar ratio was kept constant at 18, differences were observed in the extent and rate of chlorate reduction for different initial chlorate concentrations indicating that there are secondary reactions involved in the mechanisms of chlorate reduction by UV-L/sulfite that consume the reactive species formed by UV-L irradiation of sulfite solutions. Furthermore, the light intensity is maintained constant during these experiments, which can be a limiting factor for the formation of stoichiometric amounts of reactive species when high sulfite doses are used.

Fig. 4 presents the changes of chlorates decay yield with the UV-L dose measured at the end of the kinetic experiments after a reaction time of 420 min under similar operating conditions. Initial conditions for these experiments were: chlorate concentration = 10.5 mg Cl/L, sulfite dose = 180 mg/L, pH = 5.4, T = 25°C, DO = 0.21 mg O_2/L, and UV-L power output = 75 W. Chlorate decay yield increased from 51.5% for UV-L light dose of 425 µW/cm^2 to 68.3%, 77.7%, 91.5%, 99.6%, and 99.99% for UV-L light doses of 525, 585, 670, 750, and 825 µW/cm^2, respectively. This indicates that the UV-L dose affected significantly the efficacy of UV-L/sulfite ARP in eliminating chlorate from

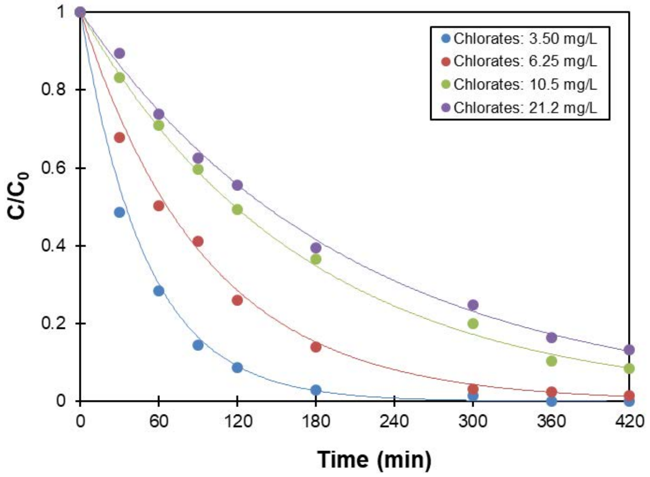

Fig. 3. Effect of initial chlorate concentration on the changes of normalized chlorate concentration (C/C_0) with time during photochemical chlorate reduction using UV-L/sulfite ARP. Experimental conditions: initial chlorate concentration: 3.50–21.2 mg/L, (sulfite/chlorate) molar ratio: 18; initial pH = 5.4; T = 25°C; DO = 0.21 mg O_2/L; UV-L power output: 75 W; UV light intensity: 670 µW/cm^2.

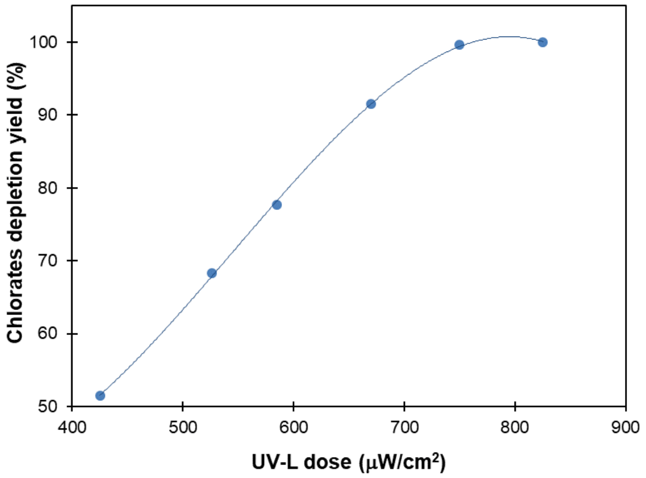

Fig. 4. Changes of chlorates decay yield with UV-L dose during chlorate photochemical reduction using UV-L/sulfite ARP. Experimental conditions: initial chlorate concentration: 10.5 mg Cl/L, sulfite dose: 180 mg/L, initial pH = 5.4, T = 25°C, DO = 0.21 mg O_2/L, UV-L power output: 75 W, UV light intensity: 425–825 µW/cm^2.

water. The increase of UV-L light dose up to 670 μW/cm^2 enhanced the efficacy of UV-L/sulfite ARP. However, higher UV-L light doses had minor improvement in the chlorate decay yield. This demonstrates that 670 μW/cm^2 is appropriately effective in activating sulfite and produces an adequate amount of reactive species able to reduce chlorate concentration to levels less than the proposed MCL.

Fig. 5 presents the measured concentrations of chlorate, chlorite, free chlorine, and chloride with time for a set of UV-L/sulfite ARP kinetic experiments. The initial conditions of these experiments were: sulfite dose = 180 mg/L, initial chlorate concentration = 10.5 mg/L (4.46 mg/L), initial pH = 5.4, DO = 0.21 mg O_2/L, UV-L power output = 75 W, and UV light intensity = 670 μW/cm^2. As it can be seen, chlorate decay is accompanied by a simultaneous formation of chloride ions from the beginning of photochemical treatment. 99% of chlorate was converted into chloride ions by UV-L/sulfite ARP after 420 min. No chlorite was detected, but a small amount of free chlorine was formed during the photochemical treatment. These results indicate that chloride ions are the major final products of chlorate reduction using UV-L/sulfite ARP. Free chlorine ($HClO/ClO^-$) ions were formed as intermediate species that were rapidly converted into chlorides and they were mostly depleted at the end of the treatment. These results reveal that the mechanism of chlorate reduction by UV-L/sulfite could involve several steps of oxygen abstraction from ClO_3^- to ClO_2^-, then from ClO_2^- to ClO^- and ends with the release of chloride ions.

Fig. 6 displays the effect of DO on the rate of chlorate reduction. As it can be seen, DO had a significant effect on both the kinetics and efficiency of chlorate reduction with UV-L/sulfite ARP. The pseudo-first-order rate constant (k_{app}) decreased from 0.006 min^{-1} when DO = 0.21 mg/L to 0.002 and 0.001 min^{-1} in presence of 6.12 and 8.50 mg/L DO, respectively. In addition, chlorate decay yield decreased from 91.5 at DO = 0.21 to 60.6% and 44.8% in presence of 6.12 and 8.50 mg/L DO, respectively (after 420 min). It was reported that molecular oxygen O_2 is a scavenger for sulfite anion radical and sulfur oxide radical [20,74,79]. The inhibition of chlorate decay in presence of dissolved oxygen is due to the quenching effect of O_2 on sulfite anion radical and sulfur dioxide radical. These results confirmed the important contribution of sulfur radical species ($SO_3^{\bullet -}$ or $SO_2^{\bullet}$) in the reduction of chlorate to chloride. Similar results were reported in the literature related to the DO effect on the dehalogenation of organic compounds [80–82], and the reduction of bromate [21], perchlorate [12], and chromium(VI) [83,84].

Fig. 7 presents the effects of nitrite, nitrate, and iron(III) on chlorate decay yield in deoxygenated and oxygenated solutions during photochemical chlorate reduction using UV-L/sulfite ARP (initial chlorate concentration: 10.5 mg/L, sulfite dose: 180 mg/L, initial pH = 5.4, UV-L power output: 75 W, UV light intensity: 670 μW/cm^2). The results show that the presence of nitrite, nitrate, and iron(III) affected the yield of chlorate decay.

Nitrite and nitrate inhibited chlorate decay in deoxygenated and oxygenated solutions. In deoxygenated solutions (DO = 0.21 mg/L), chlorate decay yield decreased from 91.5% to 78.8% and 83.6% in presence of nitrite and nitrate, respectively. In deoxygenated solutions, a similar decrease was observed in presence of nitrite and nitrate. This can be explained by the scavenging behavior of nitrite and nitrate towards the hydrated electron (e_{aq}^-) and a hydrogen atom ($H^{\bullet}$). It was reported that nitrite and nitrate react immediately with e_{aq}^- and $H^{\bullet}$ formed during UV-L irradiation of sulfite solution [Eqs. (12)–(15)] [81,85,86]:

$$NO_2^- + e_{aq}^- \rightarrow \left(NO_2^{\bullet}\right)^{2-} \qquad (12)$$

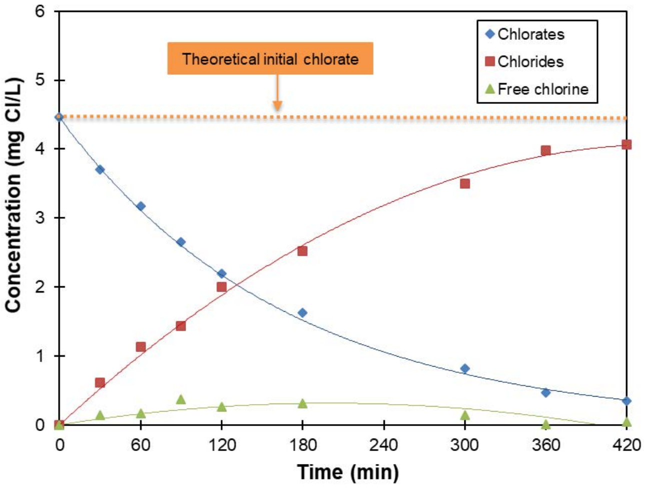

Fig. 5. Changes of chlorine species concentrations with time during photochemical chlorate reduction using UV-L/sulfite ARP. Experimental conditions: sulfite dose: 180 mg/L, initial chlorate concentration: 10.5 mg/L; initial pH = 5.4; T = 25°C; DO = 0.21 mg O_2/L; UV-L power output: 75 W; UV light intensity: 670 μW/cm^2.

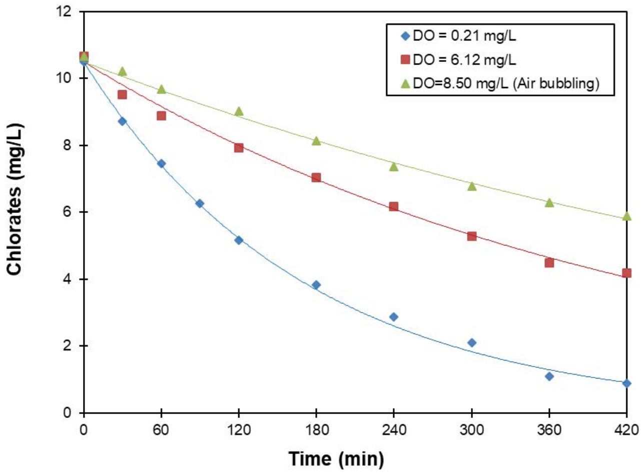

Fig. 6. Effect of dissolved oxygen (DO) on the changes of chlorate concentration with time during photochemical chlorate reduction using UV-L/sulfite ARP. Experimental conditions: initial chlorate concentration: 10.5 mg/L; sulfite dose: 180 mg/L; initial pH = 5.4; UV-L power output: 75 W; UV light intensity: 670 μW/cm^2.

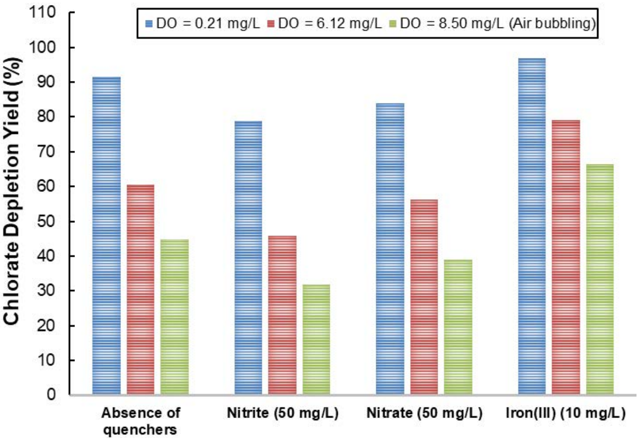

Fig. 7. Effects of nitrite, nitrate, and iron(III) (Fe^{3+}) on the chlorate decay yield in deoxygenated and oxygenated solutions during photochemical chlorate reduction using UV-L/sulfite ARP. Experimental conditions: initial chlorate concentration: 10.5 mg/L; sulfite dose: 180 mg/L; initial pH = 5.4; UV-L power output: 75 W; UV light intensity: 670 μW/cm^2).

$$NO_3^- + e_{aq}^- \rightarrow \left(NO_3^\bullet\right)^{2-} \tag{13}$$

$$NO_2^- + H^\bullet \rightarrow NO^\bullet + OH^- \tag{14}$$

$$NO_3^- + H^\bullet \rightarrow \left(HNO_3^\bullet\right)^- \tag{15}$$

These results demonstrate that hydrated electron (e_{aq}^-) and a hydrogen atom ($H^\bullet$) contribute with sulfite anion radical ($SO_3^{\bullet-}$) in the reduction of chlorate in water using UV-L/sulfite ARP.

However, the presence of Fe^{3+} enhanced chlorate decay yield in deoxygenated and oxygenated solutions. Chlorate decay yield increased from 91.5% to 96.9% in deoxygenated solutions (DO = 0.21 mg/L), and from 60.6% and 44.8% to 79.2% and 66.5% for 6.12 and 8.50 mg/L DO, respectively. It was demonstrated that Fe^{3+} can form a stable complex with HSO_3^- [87–91]. These complexes absorb UV light and decompose to form Fe^{2+} and sulfite anion radical $SO_3^{\bullet-}$ [Eqs. (16) and (17)]:

$$n HSO_3^- + Fe^{3+} \rightarrow Fe\left(HSO_3\right)_n^{(n-3)-} \tag{16}$$

$$Fe\left(HSO_3\right)_n^{(n-3)-} + h\nu \rightarrow Fe^{2+} + (n-1)HSO_3^- + H^+ + SO_3^{\bullet-} \tag{17}$$

The supplementary amount of sulfite anion radicals formed in Eq. (17) enhances the chlorate decay yield observed in presence of Fe^{3+}. This confirms the importance of sulfite anion radicals in the reduction of chlorate into chloride by oxygen atom abstraction mechanisms.

4. Conclusion

The UV-L/sulfite ARP was efficient to reduce chlorate into chloride in water under different operating conditions. The effects of sulfite dose, initial pH, initial chlorate concentration, and UV-L light intensity were evaluated. Chlorate decay followed a pseudo-first-order reaction in all conditions. The efficiency of UV-L/sulfite was high in acidic conditions when the pH value was ≤5.4 and the reaction rate constant increased with the increase of sulfite dose up to 180 mg/L for the photochemical reduction of 10 mg/L chlorate in deoxygenated solution. An increase in initial chlorate concentration resulted in a decrease in the extent and rate of chlorate reduction when sulfite/chlorate molar ratio was kept constant at 18. The increase of UV-L light dose up to 670 μW/cm^2 increased the efficiency of photochemical reduction of chlorate by UV-L/sulfite but higher doses did not show a significant improvement. Chlorate reduction was retarded in presence of dissolved oxygen due to its scavenging effect on sulfite anion radical. Also, it was retarded in the presence of nitrite and nitrate ions due to their scavenging effects on hydrated electrons. However, the presence of Fe^{3+} enhanced the efficiency of UV-L/sulfite ARP in reducing chlorate due to the additional sulfite anion radicals formed by photodecomposition of Fe^{3+}-bisulfite complexes. Based on the results obtained herein, the mechanism of chlorate reduction into chloride involves sulfite anion radical ($SO_3^{\bullet-}$), hydrated electron (e_{aq}^-), and a hydrogen atom ($H^\bullet$) through oxygen atom-abstraction sequence reactions from ClO_3^- to ClO_2^-, then to ClO^-, and end by the release of Cl^-. Accordingly, UV-L/sulfite ARP has great potential to be integrated into water and wastewater treatment processes for the removal of chlorination DBPs.

Acknowledgments

This publication was made possible by a grant from the Qatar National Research Fund under its National Priorities Research Program award number NPRP 4-1174-2-458. Its contents are solely the responsibility of the authors and do not necessarily represent the official views of the Qatar National Research Fund.

References

[1] J.L. Wang, L.J. Xu, Advanced oxidation processes for wastewater treatment: formation of hydroxyl radical and application, Crit. Rev. Env. Sci. Technol., 42 (2012) 251–325.

[2] Y. Deng, R. Zhao, Advanced oxidation processes (AOPs) in wastewater treatment, Curr. Pollut. Rep., 1 (2015) 167–176.

[3] M. Gągol, A. Przyjazny, G. Boczkaj, Wastewater treatment by means of advanced oxidation processes based on cavitation – a review, Chem. Eng. J., 338 (2018) 599–627.

[4] R. Dewil, D. Mantzavinos, I. Poulios, M.A. Rodrigo, New perspectives for advanced oxidation processes, J. Environ. Manage., 195 (2017) 93–99.

[5] M.A. Oturan, J.-J. Aaron, Advanced oxidation processes in water/wastewater treatment: Principles and applications. A review, Crit. Rev. Env. Sci. Technol., 44 (2014) 2577–2641.

[6] S. Gligorovski, R. Strekowski, S. Barbati, D. Vione, Environmental implications of hydroxyl radicals ($^\bullet$OH), Chem. Rev., 115 (2015) 13051–13092.

[7] E. Peralta, G. Roa, J.A.H. Servin, R. Romero, P. Balderas, R. Natividad, Hydroxyl radicals quantification by UV spectrophotometry, Electrochim. Acta, 129 (2014) 137–141.

[8] G.V. Buxton, C.L. Greenstock, W.P. Helman, A.B. Ross, Critical review of rate constants for reactions of hydrated electrons, hydrogen atoms and hydroxyl radicals ($^\bullet$OH/$^\bullet$O$^-$) in aqueous solution, J. Phys. Chem. Ref. Data, 17 (1988) 513–526.

[9] T. Tobien, M. Bonifaić, S. Naumov, K.D. Asmus, Time-resolved study on the reactions of organic selenides with hydroxyl and oxide radicals, hydrated electrons, and H-atoms in aqueous solution, and DFT calculations of transients in comparison with sulfur analogues, Phys. Chem. Chem. Phys., 12 (2010) 6750–6758.

[10] N. Bensalah, R. Nicola, A.A. Wahab, Nitrate removal from water using UV-M/$S_2O_4^{2-}$ advanced reduction process, Int. J. Environ. Sci. Technol., 11 (2014) 1733–1742.

[11] B.P. Vellanki, B. Batchelor, A.A. Wahab, Advanced reduction processes: a new class of treatment processes, Environ. Eng. Sci., 30 (2013) 264–271.

[12] B.P. Vellanki, B. Batchelor, Perchlorate reduction by the sulfite/ultraviolet light advanced reduction process, J. Hazard. Mater., 262 (2013) 348–356.

[13] X. Liu, B.P. Vellanki, B. Batchelor, A.A. Wahab, Degradation of 1,2-dichloroethane with advanced reduction processes (ARPs): effects of process variables and mechanisms, Chem. Eng. J., 237 (2014) 300–307.

[14] X. Liu, S. Yoon, B. Batchelor, A.A. Wahab, Degradation of vinyl chloride (VC) by the sulfite/UV advanced reduction process (ARP): effects of process variables and a kinetic model, Sci. Total Environ., 454–455 (2013) 578–583.

[15] B. Jung, A. Safan, Y. Duan, V. Kaushik, B. Batchelor, A.A. Wahab, Removal of arsenite by reductive precipitation in dithionite solution activated by UV light, J. Environ. Sci. (China), 74 (2018) 168–176.

[16] B. Jung, A. Safan, Y. Duan, V. Kaushik, B. Batchelor, A.A. Wahab, Removal of Se(IV) by the dithionite/ultraviolet advanced reduction process: effects of process variables, Environ. Eng. Sci., 35 (2018) 927–936.

[17] Y. Duan, G. Luo, B. Jung, V. Kaushik, B. Batchelor, A.A. Wahab, Photochemical degradation of arsenic and selenium with advanced reduction processes – effects of reagents, Environ. Eng. Sci., 34 (2017) 481–488.

[18] V.S.V. Botlaguduru, B. Batchelor, A.A. Wahab, Application of UV-sulfite advanced reduction process to bromate removal, J. Water Process Eng., 5 (2015) 76–82.

[19] Q. Xiao, S. Yu, L. Li, T. Wang, X. Liao, Y. Ye, An overview of advanced reduction processes for bromate removal from drinking water: reducing agents, activation methods, applications and mechanisms, J. Hazard. Mater., 324B (2017) 230–240.

[20] X. Liu, S. Yoon, B. Batchelor, A.A. Wahab, Photochemical degradation of vinyl chloride with an advanced reduction process (ARP) – effects of reagents and pH, Chem. Eng. J., 215–216 (2013) 868–875.

[21] Q. Xiao, T. Wang, S. Yu, P. Yi, L. Li, Influence of UV lamp, sulfur(IV) concentration, and pH on bromate degradation in UV/sulfite systems: mechanisms and applications, Water Res., 111 (2017) 288–296.

[22] S. Yang, Y. Zhang, D. Zheng, Advanced reduction processes: a novel technology for water treatment, Prog. Chem., 28 (2016) 934–941.

[23] B. Jung, A. Safan, V.S.V. Botlaguduru, B. Batchelor, A.A. Wahab, Impact of natural organic matter on bromate removal in the sulfite/UV-L advanced reduction process, Water Sci. Technol. Water Supply, 17 (2017) 461–471.

[24] L. Ye, H. You, J. Yao, H. Su, Water treatment technologies for perchlorate: a review, Desalination, 298 (2012) 1–12.

[25] K. Ranguelova, R.P. Mason, New insights into the detection of sulfur trioxide anion radical by spin trapping: radical trapping versus nucleophilic addition, Free Radical. Biol. Med., 47 (2009) 128–134.

[26] F.H. Getman, The ultraviolet absorption spectra of aqueous solutions of sulphur dioxide and some of its derivatives, J. Phys. Chem., 30 (1926) 266–276.

[27] M. Fischer, P. Warneck, Photodecomposition and photooxidation of hydrogen sulfite in aqueous solution, J. Phys. Chem., 100 (1996) 15111–15117.

[28] K. Hara, K. Sayama, H. Arakawa, UV photoinduced reduction of water to hydrogen in Na_2S, Na_2SO_3, and $Na_2S_2O_4$ aqueous solutions, J. Photochem. Photobiol., A, 128 (1999) 27–31.

[29] O.P. Chawla, N.L. Arthur, R.W. Fessenden, An electron spin resonance study of the photolysis of aqueous sulfite solutions, J. Phys. Chem., 77 (1973) 772–776.

[30] A.S. Jeevarajan, R.W. Fessenden, ESR studies of solvated electron in liquid solution using photolytic production, J. Phys. Chem., 93 (1989) 3511–3514.

[31] R.S. Pemberton, M.C. Depew, C. Heitner, J.K.S. Wan, Some mechanistic insights into a model bleaching process of quinones by bisulfite and dithionite: an ESR-CIDEP study, J. Wood Chem. Technol., 15 (1995) 65–83.

[32] B. Kettlitz, G. Kemendi, N. Thorgrimsson, N. Cattoor, L. Verzegnassi, Y.L.B. Collet, F. Maphosa, A. Perrichet, B. Christall, R.H. Stadler, Why chlorate occurs in potable water and processed foods: a critical assessment and challenges faced by the food industry, Food Addit. Contam., Part A, 33 (2016) 968–982.

[33] R. Aranda-Rodriguez, F. Lemieux, Z. Jin, J. Hnatiw, A.-M. Tugulea, (Yet more) challenges for water treatment plants: potential contribution of hypochlorite solutions to bromate, chlorate, chlorite and perchlorate in drinking water, J. Water Supply Res. Technol. AQUA, 66 (2017) 621–631.

[34] D. Wang, J.R. Bolton, S.A. Andrews, R. Hofmann, Formation of disinfection by-products in the ultraviolet/chlorine advanced oxidation process, Sci. Total Environ., 518–519 (2015) 49–57.

[35] S.D. Richardson, A.D. Thruston, T.V. Caughran, P.H. Chen, T.W. Collette, K.M. Schenck, B.W. Lykins Jr., C. Rav-Acha, V. Glezer, Identification of New Drinking Water Disinfection By-products from Ozone, Chlorine dioxide, Chloramine, and Chlorine, S. Belkin, Ed., Environmental Challenges, Springer, Dordrecht, 2000, pp. 95–102.

[36] S.W. Krasner, H.S. Weinberg, S.D. Richardson, S.J. Pastor, R. Chinn, M.J. Sclimenti, G.D. Onstad, A.D. Thruston, Occurrence of a new generation of disinfection byproducts, Environ. Sci. Technol., 40 (2006) 7175–7185.

[37] G. Hua, D.A. Reckhow, Comparison of disinfection byproduct formation from chlorine and alternative disinfectants, Water Res., 41 (2007) 1667–1678.

[38] A. Breytus, S. Prabakar, A.P. Kruzic, Chapter 7 – Fate of Chlorate and Perchlorate in High-Strength and Diluted Hypochlorite Solutions, K.R. Evans, E.S. Roberts-Kirchhoff, M.A. Benvenuto, K.C. Lanigan, A. Rihana-Abdallah, Eds., Trace Materials in Air, Soil, and Water, ACS Symposium Series, 2015, pp. 155–174.

[39] B.D. Stanford, A.N. Pisarenko, S.A. Snyder, G. Gordon, Perchlorate, bromate, and chlorate in hypochlorite solutions: guidelines for utilities, J. Am. Water Works Assn., 103 (2011) 71–83.

[40] S. Sorlini, F. Gialdini, M. Biasibetti, C. Collivignarelli, Influence of drinking water treatments on chlorine dioxide consumption and chlorite/chlorate formation, Water Res., 54 (2014) 44–52.

[41] X. Yang, W. Guo, X. Zhang, F. Chen, T. Ye, W. Liu, Formation of disinfection by-products after pre-oxidation with chlorine dioxide or ferrate, Water Res., 47 (2013) 5856–5864.

[42] J. Yi, Y. Ahn, M. Hong, G.H. Kim, N. Shabnam, B. Jeon, B.I. Sang, H. Kim, Comparison between OCl^--injection and in situ electrochlorination in the formation of chlorate and perchlorate in seawater, Appl. Sci., 9 (2019) 229–240.

[43] J. Radjenovic, M. Petrovic, Removal of sulfamethoxazole by electrochemically activated sulfate: implications of chloride addition, J. Hazard. Mater., 333 (2017) 242–249.

[44] E. Righi, G. Fantuzzi, G. Predieri, G. Aggazzotti, Bromate, chlorite, chlorate, haloacetic acids, and trihalomethanes occurrence in indoor swimming pool waters in Italy, Microchem. J., 113 (2014) 23–29.

[45] W.A. Jackson, A.F. Davila, D.W.G. Sears, J.D. Coates, C.P. McKay, M. Brundrett, N. Estrada, J.K. Böhlke, Widespread occurrence of (per)chlorate in the solar system, Earth Planet. Sci. Lett., 430 (2015) 470–476.

[46] R. Michalski, B. Mathews, Occurrence of chlorite, chlorate and bromate in disinfected swimming pool water, Pol. J. Environ. Stud., 16 (2007) 237–241.

[47] M. Mastrocicco, D. Di Giuseppe, F. Vincenzi, N. Colombani, G. Castaldelli, Chlorate origin and fate in shallow groundwater below agricultural landscapes, Environ. Pollut., 231 (2017) 1453–1462.

[48] H. Khasawneh, M.N. Saidan, M.A. Addous, Utilization of hydrogen as clean energy resource in chlor-alkali process, Energy Explor. Exploit., 37 (2019) 1053–1072.

[49] B. Endrődi, N. Simic, M. Wildlock, A. Cornell, A review of chromium(VI) use in chlorate electrolysis: functions, challenges and suggested alternatives, Electrochim. Acta, 234 (2017) 108–122.

[50] M.I. Gil, A. Marín, S. Andujar, A. Allende, Should chlorate residues be of concern in fresh-cut salads?, Food Control., 60 (2016) 416–421.

[51] D. Feretti, I. Zerbini, E. Ceretti, M. Villarini, C. Zani, M. Moretti, C. Fatigoni, G. Orizio, F. Donato, S. Monarca, Evaluation of chlorite and chlorate genotoxicity using plant bioassays and in vitro DNA damage tests, Water Res., 42 (2008) 4075–4082.

[52] A. Hebert, D. Forestier, D. Lenes, D. Benanou, S. Jacob, C. Arfi, L. Lambolez, Y. Levi, Innovative method for prioritizing emerging disinfection by-products (DBPs) in drinking water on the basis of their potential impact on public health, Water Res., 44 (2010) 3147–3165.

[53] Y. Garrido, A. Marín, J.A. Tudela, P. Truchado, A. Allende, M.I. Gil, Chlorate accumulation in commercial lettuce cultivated in open field and irrigated with reclaimed water, Food Control., 114 (2020) 107283–107288.

[54] K. Alfredo, B. Stanford, J.A. Roberson, A. Eaton, Chlorate challenges for water systems, J. Am. Water Works Assn., 107 (2015) E187–E196.

[55] W.P. McCarthy, T.F. O'Callaghan, M. Danahar, D. Gleeson, C. O'Connor, M.A. Fenelon, J.T. Tobin, Chlorate and other oxychlorine contaminants within the dairy supply chain, Compr. Rev. Food Sci. Food Saf., 17 (2018) 1561–1575.

[56] K. Alfredo, The potential regulatory implications of chlorate, J. Am. Water Works Assn., 107 (2014) E187–E196.

[57] S.A. Trammell, L.C.S. Lake, W.J. Dressick, Statistical evaluation of an electrochemical probe for the detection of chlorate, Sens. Actuators, B, 239 (2017) 951–961.

[58] E. Righi, P. Bechtold, D. Tortorici, P. Lauriola, E. Calzolari, G. Astolfi, M.J. Nieuwenhuijsen, G. Fantuzzi, G. Aggazzotti, Trihalomethanes, chlorite, chlorate in drinking water and risk of congenital anomalies: a population-based case-control study in Northern Italy, Environ. Res., 116 (2012) 66–73.

[59] B.I. Delpla, M.J. Rodriguez, R. Sadiq, Drinking-water management in Canadian provinces and territories: a review and comparison of management approaches for ensuring safe drinking water, Water Policy, 20 (2018) 565–596.

[60] R. Srinivasan, G. Sorial, E.S. Demessie, Removal of perchlorate and chlorate in aquatic systems using integrated technologies, Environ. Eng. Sci., 26 (2009) 1661–1671.

[61] N. Gonce, E.A. Voudrias, Removal of chlorite and chlorate ions from water using granular activated carbon, Water Res., 28 (1994) 1059–1069.

[62] P. Westerhoff, Reduction of nitrate, bromate, and chlorate by zero valent iron (Fe0), J. Environ. Eng., 129 (2003) 10–16, doi: 10.1061/(ASCE)0733–9372.

[63] C.I. Carlström, D. Loutey, S. Bauer, I.C. Clark, R.A. Rohde, A.T. Iavarone, L. Lucas, J.D. Coates, (Per)chlorate-reducing bacteria can utilize aerobic and anaerobic pathways of aromatic degradation with (Per)chlorate as an electron acceptor, MBio., 6 (2015) e02287–14.

[64] M.G. Liebensteiner, M.W.H. Pinkse, B. Nijsse, P.D.E.M. Verhaert, N. Tsesmetzis, A.J.M. Stams, B.P. Lomans, Perchlorate and chlorate reduction by the Crenarchaeon Aeropyrum pernix and two thermophilic Firmicutes, Environ. Microbiol. Rep., 7 (2015) 936–945.

[65] O. Wang, J. Coates, Biotechnological applications of microbial (Per)chlorate reduction, Microorganisms, 5 (2017) 76–84.

[66] C.G.V. Ginkel, C.M. Plugge, C.A. Stroo, Reduction of chlorate with various energy substrates and inocula under anaerobic conditions, Chemosphere, 31 (1995) 4057–4066.

[67] S. Sorlini, C. Collivignarelli, Chlorite removal with ferrous ions, Desalination, 176 (2005) 267–271.

[68] L.I. Kuznetsova, N.I. Kuznetsova, S.V. Koscheev, V.I. Zaikovskii, A.S. Lisitsyn, K.M. Kaprielova, N.V. Kirillova, Z. Twardowski, Carbon-supported iridium catalyst for reduction of chlorate ions with hydrogen in concentrated solutions of sodium chloride, Appl. Catal., A, 427–428 (2012) 8–15.

[69] D. Shuai, B.P. Chaplin, J.R. Shapley, N.P. Menendez, D.C. McCalman, W.F. Schneider, C.J. Werth, Enhancement of oxyanion and diatrizoate reduction kinetics using selected azo dyes on Pd-based catalysts, Environ. Sci. Technol., 44 (2010) 1773–1779.

[70] B. Jung, R. Sivasubramanian, B. Batchelor, A.A. Wahab, Chlorate reduction by dithionite/UV advanced reduction process, Int. J. Environ. Sci. Technol., 14 (2017) 123–134.

[71] E.W. Rice, R.B. Baird, A.D. Eaton, 4500-Cl Chlorine (Residual), Standard Methods for the Examination of Water and Wastewater, 2018, pp. 1–35.

[72] Y. Zuo, J. Zhan, T. Wu, Effects of monochromatic UV-visible light and sunlight on Fe(III)-catalyzed oxidation of dissolved sulfur dioxide, J. Atmos. Chem., 50 (2005) 195–210.

[73] Y. Zuo, J. Zhan, Effects of oxalate on Fe-catalyzed photooxidation of dissolved sulfur dioxide in atmospheric water, Atmos. Environ., 39 (2005) 27–37.

[74] A. Yazdanbakhsh, A. Eslami, G. Moussavi, M. Rafiee, A. Sheikhmohammadi, Photo-assisted degradation of 2,4,6-trichlorophenol by an advanced reduction process based on sulfite anion radical: degradation, dechlorination and mineralization, Chemosphere, 191 (2018) 156–165.

[75] Y. Gu, W. Dong, C. Luo, T. Liu, Efficient reductive decomposition of perfluorooctanesulfonate in a high photon flux UV/sulfite system, Environ. Sci. Technol., 50 (2016) 10554–10561.

[76] Y. Gu, T. Liu, Q. Zhang, W. Dong, Efficient decomposition of perfluorooctanoic acid by a high photon flux UV/sulfite process: kinetics and associated toxicity, Chem. Eng. J., 326 (2017) 1125–1133.

[77] P. Neta, R.E. Huie, Free-radical chemistry of sulfite, Environ. Health Perspect., 64 (1985) 209–217.

[78] J.C. Danilewicz, Reaction of oxygen and sulfite in wine, Am. J. Enol. Vitic., 67 (2016) 13–17.

[79] B. Xie, X. Li, X. Huang, Z. Xu, W. Zhang, B. Pan, Enhanced debromination of 4-bromophenol by the UV/sulfite process: efficiency and mechanism, J. Environ. Sci. (China), 54 (2017) 231–238.

[80] K. Yu, X. Li, L. Chen, J. Fang, H. Chen, Q. Li, N. Chi, J. Ma, Mechanism and efficiency of contaminant reduction by hydrated electron in the sulfite/iodide/UV process, Water Res., 129 (2018) 357–364.

[81] X. Li, J. Fang, G. Liu, S. Zhang, B. Pan, J. Ma, Kinetics and efficiency of the hydrated electron-induced dehalogenation by the sulfite/UV process, Water Res., 62 (2014) 220–228.

[82] L. Wang, X. Liu, Fast degradation of monochloroacetic acid by bioi-enhanced UV/S(IV) process: efficiency and mechanism, Catalysts, 9 (2019) 460–473.

[83] B. Xie, C. Shan, Z. Xu, X. Li, X. Zhang, J. Chen, B. Pan, One-step removal of Cr(VI) at alkaline pH by UV/sulfite process: reduction to Cr(III) and in situ Cr(III) precipitation, Chem. Eng. J., 308 (2017) 791–797.

[84] B. Jiang, Y. Liu, J. Zheng, M. Tan, Z. Wang, M. Wu, Synergetic transformations of multiple pollutants driven by Cr(VI)-sulfite reactions, Environ. Sci. Technol., 49 (2015) 12363–12371

[85] X. Li, J. Ma, G. Liu, J. Fang, S. Yue, Y. Guan, L. Chen, X. Liu, Efficient reductive dechlorination of monochloroacetic acid by sulfite/UV process, Environ. Sci. Technol., 46 (2012) 7342–7349.

[86] H. Herrmann, On the photolysis of simple anions and neutral molecules as sources of O^-/OH, SOx- and Cl in aqueous solution, Phys. Chem. Chem. Phys., 9 (2007) 3935–3964.

[87] C. Brandt, I. Fábián, R.V. Eldik, Kinetics and mechanism of the iron(III)-catalyzed autoxidation of sulfur(IV) oxides in aqueous solution. Evidence for the redox cycling of iron in the presence of oxygen and modeling of the overall reaction mechanism, Inorg. Chem., 33 (1994) 687–701.

[88] C. Brandt, R.V. Eldik, Kinetics and mechanism of the iron(III)-catalyzed autoxidation of sulfur(IV) oxides in aqueous solution. The influence of pH, medium and aging, Transit. Met. Chem., 23 (1998) 667–675.

[89] J. Kraft, R.V. Eldik, Kinetics and mechanism of the iron(III)-catalyzed autoxidation of sulfur(IV) oxides in aqueous solution.

2. Decomposition of transient iron(III)-sulfur(IV) complexes, Inorg. Chem., 28 (1989) 2306–2312.

[90] J. Kraft, R.V. Eldik, Kinetics and mechanism of the iron(III)-catalyzed autoxidation of sulfur(IV) oxides in aqueous solution. 1. Formation of transient iron(III)-sulfur(IV) complexes, Inorg. Chem., 28 (1989) 2297–2305.

[91] K.S. Gupta, S.V. Manoj, P.K. Mudgal, Kinetics of iron(III)-catalyzed autoxidation of sulfur(IV) in acetate buffered medium, Transit. Met. Chem., 33 (2008) 311–316.